








The Substantial Role of Cell and Nanoparticle Surface Properties in the Antibacterial Potential of Spherical Silver Nanoparticles

Marta Krychowiak-Maśnicka ^{1,*}, Weronika Paulina Wojciechowska ^{1,*}, Karolina Bogaj ¹, Aleksandra Bielicka-Giełdoń ², Ewa Czechowska³, Magdalena Ziąbka ⁴, Magdalena Narajczyk ⁵, Anna Kawiak ⁶, Tomasz Mazur⁷, Beata Szafranek², Aleksandra Królicka ¹

¹University of Gdansk, Intercollegiate Faculty of Biotechnology, Laboratory of Biologically Active Compounds, Gdansk, Poland; ²University of Gdansk, Faculty of Chemistry, Gdansk, Poland; ³University of Gdansk, Intercollegiate Faculty of Biotechnology, Laboratory of Experimental and Translational Immunology, Gdansk, Poland; ⁴AGH University of Krakow, Faculty of Materials Science and Ceramics, Department of Ceramics and Refractories, Krakow, Poland; ⁵University of Gdansk, Faculty of Biology, Bioimaging Laboratory, Gdansk, Poland; ⁶University of Gdansk, Intercollegiate Faculty of Biotechnology, Laboratory of Plant Protection and Biotechnology, Gdansk, Poland; ⁷AGH University of Krakow, Academic Centre for Materials and Nanotechnology, Krakow, Poland

*These authors contributed equally to this work

Correspondence: Marta Krychowiak-Maśnicka, Laboratory of Biologically Active Compounds, Intercollegiate Faculty of Biotechnology of the University of Gdansk and the Medical University of Gdansk, University of Gdansk, Abrahama 58, Gdansk, 80-307, Poland, Email marta.krychowiak@ug.edu.pl

Purpose: Although it is well known that the size, shape, and surface chemistry affect the biological potential of silver nanoparticles (AgNPs), the published studies that have considered the influence of AgNP surface on antibacterial activity have not provided conclusive results. This is the first study whose objective was to determine the significance of the surface net charge of AgNPs on their antibacterial potential, attraction to bacterial cells, and cell envelope disruption, considering differences in bacterial surface properties.

Methods: We evaluated five commercial AgNP colloids with identical size and shape but different surface ligands. We thoroughly characterized their physicochemical properties, including the zeta potential, hydrodynamic diameter, and polydispersity index, and determined the minimal inhibitory concentration (MIC) and minimal bactericidal concentration (MBC), along with silver absorption into bacterial cells. Moreover, we investigated structural changes in bacteria treated with AgNPs by using a crystal violet assay and electron microscopy.

Results: The zeta potential of AgNPs ranged from -47.6 to $+68.5$ mV, with a hydrodynamic diameter of 29–87 nm and a polydispersity index of 0.349–0.863. Bacterial susceptibility varied significantly ($0.5 \leq \text{MIC} \leq 256 \mu\text{g Ag/mL}$; $1 \leq \text{MBC} \leq 256 \mu\text{g Ag/mL}$); we found the lowest susceptibility in bacteria with a cell wall or a polysaccharide capsule. The most active AgNPs ($0.5 \leq \text{MIC} \leq 32 \mu\text{g Ag/mL}$; $2 \leq \text{MBC} \leq 64 \mu\text{g Ag/mL}$) had a moderate surface charge (-21.5 and $+14.9$ mV). The antibacterial potential was unrelated to ion dissolution or cell envelope disruption, and bacterial cells absorbed less of the most active AgNPs (1.75–7.65%).

Conclusion: Contrary to previous reports, we found that a moderate surface charge is crucial for the antibacterial activity of AgNPs, and that a significant attraction of the nanoparticle to the cell surface reduces the antibacterial potential of AgNPs. These findings challenge the existing views on AgNP antibacterial mechanisms and interactions with bacterial cells.

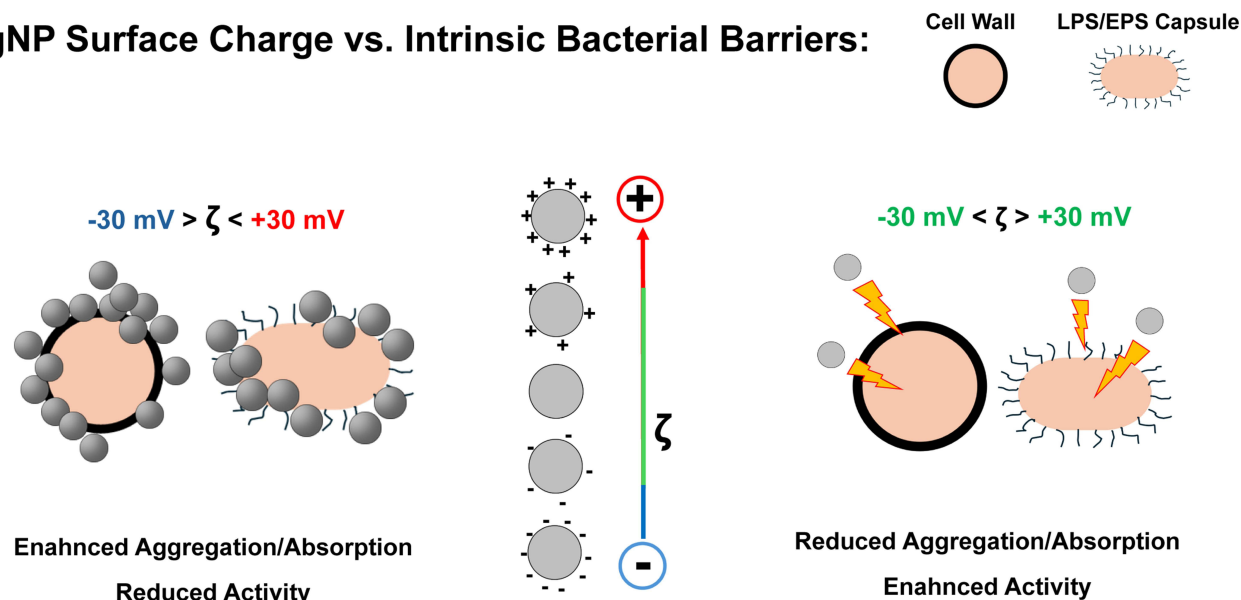
Keywords: human pathogen, ESKAPE, *Klebsiella pneumoniae*, cell envelope, ICP-OES, cell–nanoparticle interaction

Introduction

Silver nanoparticles (AgNPs) are one of the most studied species among nanoscale metal materials; they are widely used in many fields, including textiles, electronics, imaging, and nanomedicine.¹ The unique physical properties of AgNPs are due to their small size (in nanometers), high surface-to-volume ratio, and the variety of possible surface modifications. Moreover, the highly reactive cargo—silver ions—underlie the value of AgNPs in the fight against microorganisms.²

Graphical Abstract

AgNP Surface Charge vs. Intrinsic Bacterial Barriers:



According to the literature, AgNPs are broad-spectrum antimicrobials that can be exploited to combat antimicrobial-resistant bacteria.² AgNPs are also considered a source of silver, which is more active against microorganisms and less toxic than silver salts (ie, silver nitrate and silver sulfadiazine).³ There are numerous reports on the antibacterial activity of a variety of AgNPs against selected bacterial pathogens that infect humans,⁴ animals,⁵ and plants.⁶ Unfortunately, the specific processes triggered by AgNPs and their molecular targets that lead to the death of bacterial cells remain undetermined.⁷ However, many attempts, including very recent ones, have been made to understand the antibacterial mechanism of AgNPs.^{8,9} Qing et al⁷ reported multiple events that could contribute to this mechanism in bacterial cells treated with AgNPs, inter alia, an outburst of highly reactive silver ions and cell envelope disruption.⁷

Although the use of AgNPs as a source of silver is limited due to their toxicity and negative environmental impact, they remain an invaluable ingredient in wound care products.^{10,11} The potential of silver ions to reduce the microbial burden is essential to control infections that impair the healing process and remains highly relevant for managing chronic wounds, cases of which are on the rise due to population aging, accompanied by an increasing prevalence of lifestyle diseases and microbial resistance to antibiotics.¹² Hence, AgNPs have been intensively studied, and the number of reports on potential, new methods to synthesize and implement them into wound-healing materials has increased steadily over time.

The antimicrobial activity of AgNPs has been investigated in several experimental studies, which have concluded that they have a wide range of antimicrobial potential. However, according to PubMed, most of these studies have focused on three human pathogens: *Escherichia coli*, *Staphylococcus aureus*, and *Pseudomonas aeruginosa*. Moreover, most studies have been designed to test the biological activity of either a specific AgNP colloid tested against selected bacterial species or a range of AgNP colloids against a particular bacterial pathogen.^{2,4,8} None of these studies considered significant differences in bacterial cell surface properties. Furthermore, many scientific publications have emphasized that size, shape, and surface play a crucial role in the biological activity of AgNPs.^{2,3,8,13} Of note, there is an ongoing debate on the recommended properties of AgNPs. Numerous researchers have investigated the role of surface net charge in the antibacterial potential of AgNPs, but the conclusions have been equivocal: Either a negative^{14–16} or a positive^{17–20} surface net charge determines their antibacterial activity. Therefore, the objective of the study was to investigate the influence of the nanoparticle surface net charge and bacterial surface properties on the antibacterial potential of AgNPs.

A novel concept of this study was the use of thoroughly characterized AgNPs that varied in their surface charge from highly negative to highly positive and evaluation of a range of selected pathogens representing gram-positive (G-pos) and gram-negative (G-neg) bacteria with distinct cell surface properties. Moreover, the attraction of AgNPs to bacterial cells and cell envelope disruption induced by nanoparticles were studied to evaluate the significance of the nanoparticle charge on these antibacterial mechanisms.

Materials and Methods

Materials

Silver nitrate (> 99% purity) was purchased from Merck Sp. z o.o. (Warsaw, Poland). The following criteria were applied to select AgNP colloids: (i) reputable provider(s), ensuring consistency and reproducibility, (ii) identical size and shape of nanoparticles to avoid the influence of parameters other than surface properties, and (iii) varying surface chemistry and ionic character of the surface ligand (cationic, anionic, neutral) to obtain a broad gradient of surface net charge. Based on these criteria, the following commercial colloids of spherical AgNPs ($\text{\O} \approx 5 \text{ nm}$) were used: (i) AgNPs-NMe₃⁺ stabilized with (11-mercaptoundecyl)-*N,N,N*-trimethylammonium chloride (cat. no. NP CI 007), (ii) AgNPs-C10COOH stabilized with mercaptoundecanoic acid (cat. no. NP CI 003), (iii) AgNPs-EG3OH stabilized with triethylene glycol mono-11-mercaptoundecyl ether (cat. no. NP BR 005), (iv) AgNPs-Cit coated with sodium citrate (cat. no. AGPB5), and (v) AgNPs-PVP coated with polyvinylpyrrolidone (catalog no. AGCB5). AgNPs-NMe₃⁺, AgNPs-C10COOH, and AgNPs-EG3OH were purchased from Prochimia Surfaces sp. z o.o. (Sopot, Poland). AgNPs-Cit and AgNPs-PVP were purchased from NanoComposix (San Diego, CA, USA).

The following microbiological media were used: Brain-Heart Infusion (BHI) broth and Cation-Adjusted Mueller-Hinton Broth (CA-MHB, pH 7.3) from Becton Dickinson (Franklin Lakes, NJ, USA), and Trypticase Soy Agar (TSA) from BTL Sp. z o.o. (Łódź, Poland). Phosphate-buffered saline (PBS, pH 7.4), crystal violet (CV) of $\geq 99.7\%$ purity, and phenylalanine-arginine β -naphthylamide dihydrochloride (PA β N) of $\geq 98\%$ purity were purchased from Merck Sp. z o.o. (Warsaw, Poland). Lysostaphin (0.4 U/ μ L) was purchased from A&A Biotechnology (Gdańsk, Poland). Commercially available fresh, defibrinated sheep blood (sold as media supplement) was purchased from GRASO[®] Biotech (Owidz, Poland). RPMI 1640 medium (Gibco[®], pH 7.0–7.4) was obtained from Thermo Fisher Scientific (Waltham, MA, USA). Antibacterial tests were performed in sterile, polystyrene, flat-bottom 96-well plates for non-adherent cultures (Merck Sp. z o.o., Warsaw, Poland), whereas fluorescence measurements were performed in black microplates with transparent bottoms (Thermo Fisher Scientific). Ultrapure water (PURELAB[®] ELGA system, High Wycombe, UK) was used to prepare buffers and liquid media for bacterial cultures and to perform measurements aiming to characterize AgNPs.

Bacterial Species

Six strains representing bacterial species characterized by a high frequency of antimicrobial resistance²¹ were used throughout the study: *Staphylococcus aureus* ATCC 25923, *Enterococcus faecalis* ATCC 19433, *Escherichia coli* ATCC 25922, *Pseudomonas aeruginosa* ATCC 27853, *Acinetobacter baumannii* ATCC 19606, and *Klebsiella pneumoniae* ATCC 700603. *S. aureus* and *E. faecalis* represent G-pos bacteria with thick cell wall on the cell surface, whereas *E. coli*, *P. aeruginosa*, *A. baumannii*, and *K. pneumoniae* are G-neg bacteria with outer cell membrane enveloping the cell. Additionally, *K. pneumoniae* is known for its thick extracellular polysaccharide capsule.²¹

Antibacterial Potential

The concentration of silver in the AgNP colloids was determined using inductively coupled plasma optical emission spectrometry (ICP-OES) according to the method described previously.²² The standard broth microdilution method was applied using the methodology described previously,²² with slight modifications. All bacterial cultures were performed on TSA plates (24 h, 37 °C) and in BHI broth (5 h, 37 °C, 130 rpm), and antibacterial tests were performed in 96-well plates in CA-MHB (24 h, 37 °C). The tested concentrations of silver sources ranged from 1 to 128 μ g Ag/mL, and were reduced or increased for more or less active agents, respectively. Bacterial cells were added to the medium immediately after the mixture with the silver source was prepared. For each silver source, two parameters were measured in two

separate experiments according to the Clinical & Laboratory Standards Institute (CLSI) guidelines, that is, the minimal inhibitory concentration (MIC) and the minimal bactericidal concentration (MBC). The MIC, defined as the minimal concentration of an agent that inhibits the growth of bacterial cells after incubation for 24 h at 37 °C, was determined for initial bacterial suspensions in a microplate with approximately 1×10^6 colony forming units (cfu)/mL. The MBC, the minimal concentration of an agent that reduces the initial number of bacterial cells by 3 logarithms after incubation for 24 h at 37 °C, was assessed for bacterial suspension in a microplate with a microbial count of about $2.5\text{--}5 \times 10^5$ cfu/mL. Each concentration was tested in triplicate, and the entire experiment was repeated three times to define the median MIC and MBC.

AgNP Characteristics

Transmission electron microscopy (TEM) was employed to determine the shape and the average size of the NPs in the tested samples. AgNP colloids (2 μ L) were placed on a Formvar/Carbon-Supported Copper Grid, 300 mesh (EM Resolutions, New Castle, UK) and air-dried. The samples were examined using a Tecnai G2 Spirit BioTWIN electron microscope (FEI Company, Hillsboro, OR, USA) at 120 kV. The size of the nanoparticles in the tested colloids was measured manually from transmission electron micrographs ($n \geq 380$ nanoparticles) and calculated considering the scale bar. Ultraviolet–visible (UV–Vis) spectra were obtained for AgNP suspensions in ultrapure water (10 μ L in 1 mL) using a Specord 200 Plus spectrophotometer (Analytik Jena, Jena, Germany). The size distribution of the particles in the colloids was measured using a Nano S Zetasizer system (Malvern PANalytical, Malvern, UK) and used to determine the average hydrodynamic diameter, the polydispersity index (PDI), and size distribution by volume. The parameters were calculated with the Malvern Zetasizer software (version 7.13) dedicated for the equipment. The measurement parameters were as follows: laser wavelength, 633 nm (He–Ne); scattering angle, 173°; measurement temperature, 25 or 37 °C; medium viscosity, 0.8872 mPa·s; medium refractive index 1.330; and material refractive index, 0.14. A multiple narrow-mode algorithm (with high resolution) was applied. Five measurements were performed.

The zeta (ζ) potential of the AgNPs in the tested colloids was measured using a particle size analyzer (Litesizer™ 500, Anton Paar, Graz, Austria). Each sample was measured three times at 25 °C, and each measurement was performed immediately after the sample was diluted in ultrapure water and placed in disposable omega-shaped cuvettes (Anton Paar). The concentration of the sample applied during the experiment was defined empirically to achieve optimal conductivity (0.01–1 mS/cm). The ζ potential and size distribution of the nanoparticles were measured in ultrapure water to compare the results obtained from the present study with the results obtained from previous studies, and to simplify the research model because neither the buffer (PBS) nor medium (CA-MHB) reflects the conditions during the actual antibacterial assay. In other words, both media lack bacterial cells interacting with AgNPs.

Dissolution Rate of Silver from AgNPs

To determine the susceptibility of AgNP colloids to the dissolution of silver ions, spectrophotometric measurements were conducted according to the method described by Ho et al²³ with modifications. The measurements were performed in disposable polystyrene cuvettes (Sarstedt, Nümbrecht, Germany) using a Specord 200 Plus spectrophotometer (Analytik Jena). An aliquot of a particular AgNP colloid with an equivalent of approximately 25 μ g of silver was mixed with 0.9 mL of ultrapure water. The final volume of the sample in the cuvette was adjusted to 1 mL using ultrapure water. UV–Vis spectra (300–800 nm) were recorded for each sample to determine the maximum absorption wavelength (λ_{max}). Each initial colloid (~ 25 μ g Ag/mL) was diluted in ultrapure water to obtain a gradient of the following concentrations: 12.5, 6.25, 3.125, 1.6, and 0.8 μ g Ag/mL. A linear regression model was used to define the correlation between the absorbance and concentration of AgNPs (silver equivalent) in the cuvette. The determined formulae were used in the second part of the experiment to calculate the concentration of nanoparticles (silver equivalent) in the sample after titration with hydrogen peroxide (0.004–3 M). Finally, the results were used to calculate the concentration of hydrogen peroxide dissolving 50% of AgNPs (DC50). Each colloid was tested once, and the entire experiment was performed in triplicate.

Absorption of Silver Onto Bacterial Cells

Approximately 15 bacterial colonies from a TSA plate (24 h, 37 °C) were picked with a sterile loop and used to inoculate 5 mL of BHI medium in a 50 mL conical tube (Sarstedt). After incubation for 5 h (37 °C, 130 rpm), the bacterial cultures were centrifuged for 10 min at 2800 rpm at room temperature (Eppendorf, Hamburg, Germany). The supernatant was removed immediately, and the cell pellet was resuspended in sterile PBS (0.5 mL). Then, small aliquots of concentrated bacterial suspension were transferred to 10 mL of fresh buffer to obtain an optical density equal to 2.5 McFarland standard (McF) measured with an EMO DensiMeter II (Erba Lachema, Brno-Řečkovice a Mokrá Hora, Czech Republic) and corresponding to approximately 5×10^8 cfu/mL. Next, 1-mL aliquots of the bacterial suspension were transferred to 1.5-mL polypropylene tubes (Sarstedt). Each silver source was added to the tube at a final concentration of approximately 30 µg Ag/mL. Then, the tubes were placed horizontally and incubated at 37 °C for 45 min. After incubation, the bacterial cells treated with AgNP colloids were centrifuged (10 min, 2800 rpm), the supernatant was removed, and the collected pellets were stored at -20 °C for further analyses. The bacterial pellets were dissolved in 1 mL of concentrated nitric acid and diluted in 4 mL of deionized water. ICP-OES was performed according to the method described previously.²² Tubes with a silver source suspended in buffer without bacterial cells were prepared to measure the exact initial amount of silver in the samples. Finally, the level of silver absorbed was calculated according to the equation $A_{Abs} = (A_{Pel}/A_{Total}) \times 100\%$, where A_{Abs} is the percentage of silver absorbed by cells, A_{Pel} is the amount of silver absorbed by cells measured with ICP-OES, and A_{Total} is the initial amount of silver measured by ICP-OES. Each bacterial strain was challenged with each silver source in triplicate, and the entire experiment was repeated twice.

Disruption of the Bacterial Cell Envelope

CV was used to measure the disrupting potential of the silver sources on the bacterial cell envelope according to the method described by Halder et al²⁴ and slightly modified to adjust to G-pos *S. aureus* and G-neg *E. coli*. Briefly, a 1-mL aliquot of overnight bacterial culture (37 °C, 130 rpm) was transferred to 50 mL of CA-MHB and incubated for 6 h (37 °C, 130 rpm). Then, the culture was centrifuged (5 min, 2800 g), and the collected pellet was resuspended in PBS to an optical density of 5 McF. The bacterial suspension (500 µL) was added to a 1.5-mL polypropylene tube, mixed with previously prepared solutions of silver salt or suspensions of AgNPs in PBS, and incubated for 1 h (37 °C) in a horizontal position. The silver formulations were tested at the MICs previously established for a particular pathogen. The following positive controls were applied: (i) the cell wall-disrupting enzyme lysostaphin (0.4 U/mL), exclusively for *S. aureus*, and (ii) the outer membrane-perturbing peptidomimetic compound PAβN (256 µg/mL), exclusively for *E. coli*. Next, 10 µL of CV solution in ethanol (1 mg/mL) was added to the tube, mixed well, and the sample was centrifuged immediately (15 min, 13400 g). An aliquot (100 µL) of a sample was transferred to a transparent 96-well plate, and the absorbance of CV was measured (590 nm). Disruption of the cell envelope results in contrasting effects on CV absorption into G-neg and G-pos bacterial cells, that is, uptake is enhanced and inhibited, respectively. Thus, to calculate the level of cell surface damage, the following formulas were used: (i) $D = 100 - ([A_S - A_{PBS}] / [A_{CV} - A_{PBS}]) \times 100\%$ for G-neg bacteria and (ii) $D = ([A_S - A_{PBS}] / [A_{CV} - A_{PBS}]) \times 100\%$ for G-pos bacteria, where D is the level of cell envelope disruption, A_{PBS} is the absorbance of pure PBS, A_S is the absorbance of the sample (bacterial cells untreated or treated with a silver source and then with CV), and A_{CV} is the absorbance of CV dissolved in PBS buffer (10 µg/mL). Each silver source was tested in three technical replicates, and the experiment was performed twice.

Electron Microscopy of Bacterial Cells

Late logarithmic bacterial cultures in CA-MHB (6 h, 130 rpm, 37 °C) were diluted with fresh medium (5 McF). Aliquots (1 mL) of the cultures were transferred to 2-mL tubes, and silver sources were added (8× MIC). After incubation for 1 h, the samples were centrifuged (10 min, 2800 g) and the pellet was resuspended in 100 µL PBS. For scanning electron microscopy (SEM), 2-µL aliquots of bacterial suspension were placed immediately onto two Formvar/Carbon-Supported Copper Grids, 300 mesh (EM Resolutions, Keele, UK), and air-dried samples were analyzed with a Nova Nano SEM 200 (FEI Company, Hillsboro, OR, USA) in a low vacuum in the secondary electron mode using the HELIX detector. For TEM, samples were fixed with 2.5% glutaraldehyde (Polysciences, Warrington, PA, USA) and post-fixed with 1%

osmium tetroxide (Agar Scientific, Stansted, UK) in PBS. After dehydration in a graded series of ethanol solutions, the samples were embedded in Epon resin (Merck Sp. z o.o., Warsaw, Poland). Ultrathin sections were cut using a Leica UC7 ultramicrotome (Leica Microsystems, Wetzlar, Germany), stained with UranylLess (Delta Microscopies, Mauressac, France) and Reynold's lead citrate (Delta Microscopies), and examined using a Tecnai G2 Spirit BioTWIN electron microscope (FEI Company) at 120 kV.

Hemolytic Activity

Hemolysis was measured according to the method described by Zhao et al,²⁵ with slight modifications. Sheep blood was diluted in RPMI 1640 medium (2% v/v) and aliquots (500 μ L) were transferred to 2-mL tubes and mixed with 500 μ L of a particular silver source in RPMI 1640 medium. A concentration gradient of the silver salt and AgNP colloids was applied (128 to 1 μ g Ag/mL). After incubation for 1 h at 37 °C, the samples were centrifuged (4 °C, 8 min, 10000g), and 200- μ L aliquots were transferred to transparent 96-well plates. The absorbance of hemoglobin (540 nm) was measured using the EnVision microplate reader (PerkinElmer, Waltham, MA, USA). Untreated blood in the medium was used as a negative control (0% hemolysis), whereas blood treated with sodium dodecyl sulfate (SDS; 50 μ g/mL) was used as a positive control (100% hemolysis). The hemolysis level was calculated according to the following formula: $H = ([A_S - A_{RPMI}] / [A_{SDS} - A_{RPMI}]) \times 100\%$, where H is the hemolysis level (%), A_S is the absorbance of the sample, A_{RPMI} is the absorbance of the medium after centrifugation of untreated blood cells, and A_{SDS} is the absorbance of the cell suspension treated with SDS. The results were used to prepare a calibration curve and to calculate the HC50, that is, the concentration of each silver source leading to 50% hemolysis. Each silver source was tested in one replicate, and the entire experiment was performed in triplicate.

Cytotoxicity Toward Eukaryotic Cells

The 3-[4,5-dimethylthiazol-2-yl]-2,5 diphenyl tetrazolium bromide (MTT) assay was employed to assess the cytotoxicity of silver nitrate and selected AgNPs toward normal, non-malignant HaCaT cells according to the method described in a previous publication.²⁶ AgNP colloids were applied at a concentration gradient—from 128 to 1 μ g Ag/mL—whereas silver nitrate concentrations ranged from 0.5 to 16 μ g Ag/mL. The results were used to calculate the IC50, that is, the concentration of the tested agent that reduced the cell viability by 50%. Each silver source concentration was tested in one replicate, and the entire experiment was repeated three times.

Statistical Analyses

The statistical significance of the obtained results was analyzed using SPSS Statistics 29 (IBM, Armonk, NJ, USA). Each applied statistical test is described in detail for the particular dataset discussed in the text. The significance level was set at $\alpha = 0.05$.

Results

Physical Properties of AgNPs

We performed a series of analyses to fully characterize the AgNP colloids selected for this study. The water suspensions of all tested AgNPs presented their maximum absorbance peaks within the range of 390–430 nm ([Supplementary Figure 1, right panel](#)), typical for AgNPs. Although TEM confirmed that spherical particles with a diameter of 5 nm were present in all samples, all colloids were characterized by slightly different size distributions ([Supplementary Figure 1, left and middle panel](#)). The average size of the metal core in the tested colloids determined from the transmission electron micrographs was 4 nm for AgNPs-NMe3⁺; 5 nm for AgNPs-Cit, AgNPs-C10COOH, and AgNPs-EG3OH; and 6 nm for AgNPs-C10COOH ([Supplementary Table 1](#)). Moreover, AgNPs-C10COOH and AgNPs-EG3OH presented greater variability in size compared with the other tested colloids ([Supplementary Table 1](#)). The average hydrodynamic diameter based on the volume of nanoparticles varied from 2 ± 0.4 nm for AgNPs-NMe3⁺ to 47 ± 13 nm for AgNPs-PVP ([Supplementary Table 1](#)). AgNPs-C10COOH and AgNPs-PVP had a similar hydrodynamic diameter, that is, 35 ± 9 nm and 47 ± 13 nm, respectively; the hydrodynamic diameter of AgNPs-Cit and AgNPs-EG3OH was also comparable— $9 \pm$

2 nm and 13 ± 7 nm, respectively ([Supplementary Table 2](#)). Although AgNPs-NMe₃⁺ had a smaller hydrodynamic diameter compared with the other AgNP colloids (2 ± 0.4 nm), the differences in the hydrodynamic diameter of the others were resulting from different surface ligands, that is, their size and the size of the solvent molecule layer. The PDI ([Supplementary Table 1](#)), calculated by the software based on the intensity of nanoparticles, revealed that the size of AgNPs-EG3OH and AgNPs-NMe₃⁺ is more dispersed (PDI = 0.691 and 0.580, respectively) compared with AgNPs-Cit, AgNPs-C10COOH, and AgNPs-PVP (PDI of 0.229–0.292). The ζ potential was measured to determine the net surface charge of the applied nanoparticles. It ranged from -47.6 ± 0.8 mV for AgNPs-Cit to $+68.5 \pm 2.2$ mV for AgNPs-NMe₃⁺ ([Supplementary Table 1](#)). Finally, all tested colloids added to media (CA-MHB and RPMI 1640) formed clear suspensions, without visible aggregates or precipitates at the start of the experiment.

Species-Dependent Antibacterial Susceptibility to Silver

We used a solution of silver nitrate and five AgNP colloids to investigate the susceptibility of selected bacterial species to different sources of silver. The results are summarized in [Supplementary Table 2](#). Although all six bacteria were susceptible to silver nitrate, the effective doses of ionic silver differed slightly among the species. *P. aeruginosa* was most sensitive to silver ions (MIC = 0.5 $\mu\text{g Ag/mL}$, MBC = 1 $\mu\text{g Ag/mL}$), followed by *E. faecalis* and *E. coli* (MIC = 2 $\mu\text{g Ag/mL}$, MBC = 4 $\mu\text{g Ag/mL}$); and *S. aureus*, *A. baumannii*, and *K. pneumoniae* ($2 \leq \text{MIC} \leq 4 \mu\text{g Ag/mL}$, MBC = 8 $\mu\text{g Ag/mL}$). The MBC-to-MIC ratio (≤ 4) indicated the bactericidal potential of silver nitrate against the six tested pathogens.

The analyses also revealed significant differences in bacterial susceptibility to AgNPs ([Supplementary Table 2](#)). We compared the MICs for the tested AgNP colloids with the MICs for silver nitrate ($\leq 4 \mu\text{g Ag/mL}$) to define the following arbitrary breakpoints: MIC $\leq 4 \mu\text{g Ag/mL}$ for sensitivity, $8 \leq \text{MIC} \leq 32 \mu\text{g Ag/mL}$ for moderate sensitivity, and MIC $\geq 64 \mu\text{g Ag/mL}$ for resistance. There were distinct patterns of sensitivity among the six tested species: *E. coli* and *P. aeruginosa* were sensitive to all AgNPs (MIC $< 4 \mu\text{g Ag/mL}$); *S. aureus*, *E. faecalis*, and *A. baumannii* were sensitive to some AgNP colloids and moderately sensitive to others; and *K. pneumoniae* presented MICs ranging from 4 to 256 $\mu\text{g Ag/mL}$.

Although the MBCs revealed a similar pattern of bacterial susceptibility among the species, there was a significant difference between G-pos and G-neg bacteria in their vulnerability to AgNPs ([Supplementary Table 2](#)). For G-pos bacteria, in addition to higher MICs for the AgNP colloids, the MBC-to-MIC ratios were higher (2–16) compared with G-neg bacteria (2–4), indicating a reduction or lack of bactericidal potential of AgNPs toward G-pos bacteria.

Interestingly, we did not observe any correlation between the bacterial sensitivity to silver nitrate and susceptibility to AgNPs. In contrast, within either G-neg or G-pos bacteria, the species that were more sensitive to silver ions—that is, *P. aeruginosa* and *S. aureus*—were less susceptible to AgNPs than the species with reduced susceptibility to silver ions—that is, *E. coli* and *E. faecalis* ([Supplementary Table 2](#)). Moreover, the effective doses of AgNPs were usually higher than the effective doses of silver nitrate, with only a few exceptions: AgNPs-EG3OH for *S. aureus*, *E. coli*, and *A. baumannii*, and AgNPs-Cit or AgNPs-PVP for *E. coli*.

Although the effective doses of AgNPs ranged widely from 0.5 to 256 $\mu\text{g Ag/mL}$ for the MIC and from 1 to 256 $\mu\text{g Ag/mL}$ for the MBC ([Supplementary Table 2](#)), we observed a similar pattern for most bacterial strains. Specifically, AgNPs-EG3OH and AgNPs-PVP (or one of them) were the most active colloids ($0.5 \leq \text{MIC} \leq 32 \mu\text{g Ag/mL}$; $2 \leq \text{MBC} \leq 64 \mu\text{g Ag/mL}$), and AgNPs-C10COOH possessed the lowest antibacterial activity (MIC and MBC between 4 and 256 $\mu\text{g Ag/mL}$).

The Influence of Nanoparticle Properties on the Antibacterial Potential

We log-transformed the MBC and MIC data collected for all silver sources and bacterial strains ([Figure 1](#)) to investigate the relationship between antibacterial activity and AgNP properties ([Supplementary Table 1](#)). Neither the average core size and hydrodynamic diameter of the nanoparticles in the tested samples nor the polydispersity of the colloids correlated with the antibacterial potential of the tested nanoparticles ([Figure 1](#), [Supplementary Table 2](#), and [Supplementary Figure 2](#)). All three parameters differed among the tested colloids, but there was no pattern between their values and the antibacterial potential ([Figure 1](#)). Although we did not observe a linear correlation between the ζ

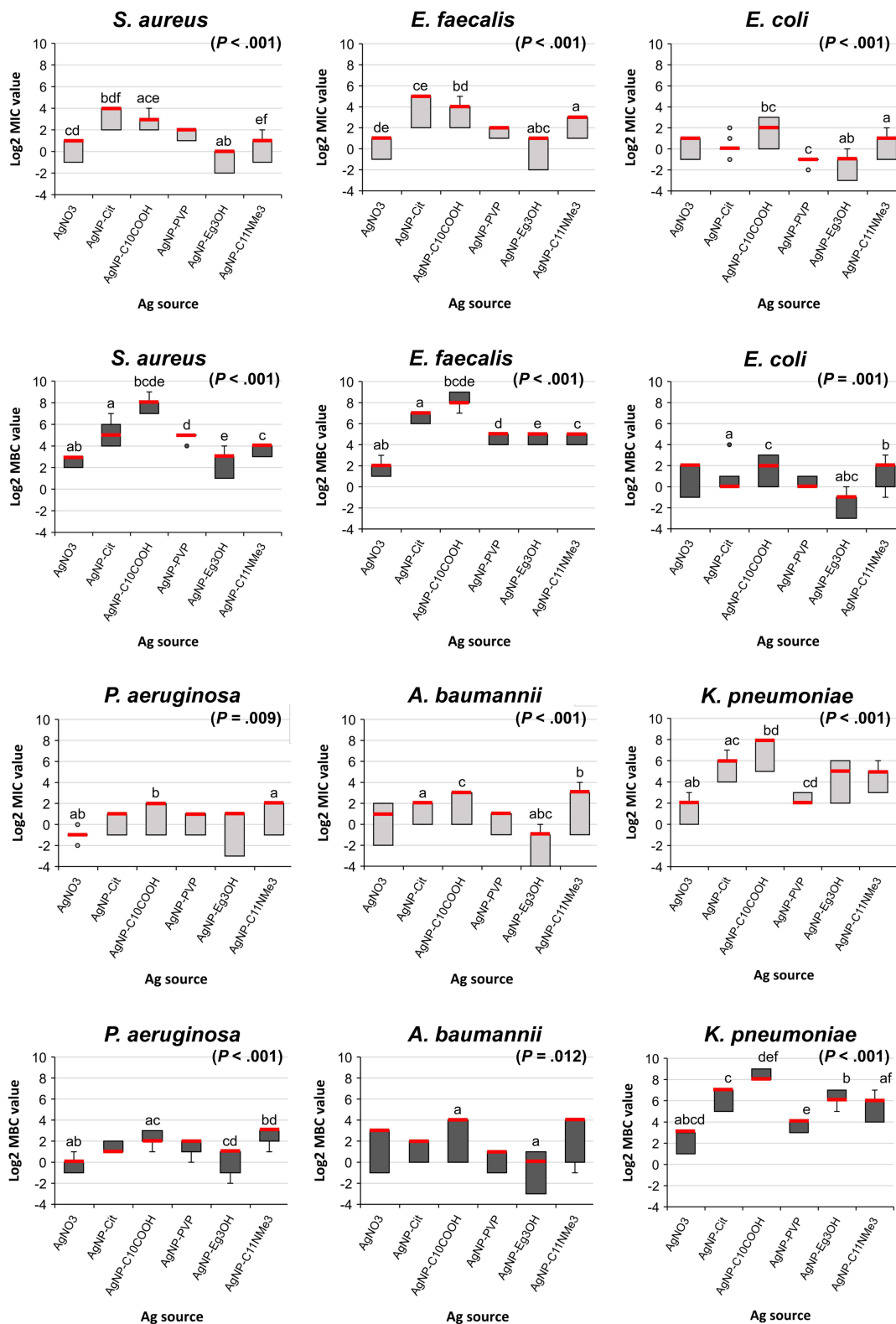


Figure 1 Statistical analysis of the inhibitory ($\log_2\text{MIC}$) and bactericidal ($\log_2\text{MBC}$) potential of silver nanoparticles (AgNPs). AgNPs are displayed in order according to the increase in the zeta potential. The results for each sample are reported as a distribution of the \log_2 -transformed MIC or MBC obtained from nine replicates. The median is marked red. Annotation in brackets represents the P -value calculated with the Kruskal–Wallis test for each set of independent groups. The values with the same letters are significantly different according to post hoc Dunn's test with Bonferroni correction ($P < \alpha$, $\alpha = 0.05$). AgNPs-Cit, AgNPs stabilized with sodium citrate. AgNPs-C10COOH, AgNPs stabilized with mercaptoundecanoic acid. AgNPs-PVP, AgNPs stabilized with polyvinylpyrrolidone. AgNPs-EG3OH, AgNPs stabilized with triethylene glycol mono-11-mercaptopdecyl ether. AgNPs-NMe3+, AgNPs stabilized with (11-mercaptopdecyl)-*N,N,N*-trimethylammonium chloride.

potential ([Supplementary Table 1](#)) and bacteriostatic or bactericidal activity ([Figure 1](#)), there was a tendency for significantly higher antibacterial activity for nanoparticles with a moderate ζ potential—that is, either -21.5 ± 0.5 mV (AgNPs-PVP) or $+14.9 \pm 0.3$ mV (AgNPs-EG3OH)—compared with more negatively or positively charged AgNPs. Moreover, we observed an interesting difference in the susceptibility of the G-pos bacteria and most of the G-neg bacteria to AgNPs with a highly negative or positive charge ([Figure 1](#)). The G-pos bacteria *S. aureus* and *E. faecalis* were significantly more vulnerable to positively charged AgNPs-NMe₃⁺ ($+68.5$ mV) compared with negatively charged AgNPs-Cit (-47.6 mV). Conversely, most of the G-neg bacteria (*E. coli*, *P. aeruginosa*, and *A. baumannii*) were inhibited or killed when exposed to significantly lower concentrations of negatively charged AgNPs-Cit compared with positively charged AgNPs-NMe₃⁺ ([Figure 1](#)). The G-neg bacterium *K. pneumoniae* produced interesting results ([Figure 1](#)): The outcome was similar to the G-pos bacteria, and the MIC or MBC of AgNPs-Cit were higher compared with AgNPs-NMe₃⁺ ([Figure 1](#)).

We determined two additional physical properties—nanoparticle aggregation and dissolution of silver ions—to assess the colloidal stability of the tested AgNPs. Although there was a wide range for the ζ potential of the tested AgNPs, that is, from highly negative (below -30 mV) to highly positive (above $+30$ mV), we observed only slight aggregation of AgNPs-C10COOH, AgNPs-PVP, and AgNPs-EG3OH at 25 °C ([Supplementary Figure 2, left panel](#), and [Supplementary Table 2](#)), and it was not elevated after incubation at 37 °C for 1 h ([Supplementary Figure 2, right panel](#)). Although the histograms of all tested colloids showed slight changes in the nanoparticle distribution at 37 °C ([Supplementary Figure 2, right panel](#)) compared with 25 °C ([Supplementary Figure 2, left panel](#)), these changes did not exceed the initial size range. At the same time, we found that the most active and moderately charged colloids, namely AgNPs-PVP (-21.5 mV) and AgNPs-EG3OH ($+14.9$ mV), showed opposite susceptibilities to hydrogen peroxide, and the dissolution rate of silver ions from AgNPs depended strictly on the negative and positive net charges of the nanoparticles ([Figure 2](#)). All negatively charged AgNPs dissolved rapidly when titrated with hydrogen peroxide, whereas positively charged nanoparticles were susceptible to high concentrations of hydrogen peroxide ([Figure 2](#)). The DC₅₀ varied slightly among the negatively charged nanoparticles (37 ± 3 mm for AgNPs-Cit, 16 ± 5 mm AgNPs-C10COOH, and 8 ± 1 mm AgNPs-PVP) and was significantly higher for the positively charged AgNPs (718 ± 162 mm for AgNPs-EG3OH and 3467 ± 1986 mm for AgNPs-NMe₃⁺). Because the DC₅₀ for the moderately charged and most active AgNPs-PVP and AgNPs-EG3OH differed significantly, there was no correlation between the antibacterial potential of AgNPs and their susceptibility to dissolution.

Silver Absorption from AgNPs with Different Surface Properties

We measured the amount of silver that penetrated the bacterial cells and attached to their surface to determine whether the surface properties of AgNPs influence the absorption of silver and, hence, determine the antibacterial activity. [Figure 3](#) shows the results of the analyses for all bacterial strains treated with silver nitrate or AgNP colloids. Although there were significant differences in silver uptake among the bacterial species when applying silver nitrate ([Figure 3](#)), the amount of absorbed silver did not correlate with the inhibitory or bactericidal doses of silver salt ([Figure 1](#) and [Supplementary Table 2](#)).

Similarly, we did not observe a positive correlation for AgNP colloids ([Figure 3](#)), that is, the most active AgNPs-PVP and AgNPs-EG3OH ([Figure 1](#) and [Supplementary Table 2](#)) were absorbed at a significantly lower level (from $1.75\% \pm 0.5\%$ to $7.65\% \pm 3.7\%$) compared with the other AgNPs (from $3.97\% \pm 0.5\%$ to $96.05\% \pm 3.82\%$). However, reduced silver absorption was not the primary determinant of the antibacterial potential of AgNPs. For example, *S. aureus* ([Figures 1](#) and [3](#)) remained vulnerable to highly absorbed AgNPs-NMe₃⁺ ($42.43\% \pm 6.55\%$), *E. faecalis* ([Figures 1](#) and [3](#)) was highly resistant to weakly absorbed AgNPs-C10COOH ($2.90\% \pm 1.24\%$), and significant differences in silver absorption profiles did not correlate with the similar susceptibility to all AgNP colloids we observed for *E. coli* and *P. aeruginosa* ([Figures 1](#) and [3](#)).

Envelope-Disrupting Potential of AgNPs with Different Surface Properties

We measured the release and uptake of CV by bacterial cells treated with the tested AgNP colloids to evaluate the role of nanoparticle-induced disruption of the cell surface in the antibacterial potential. [Figure 4](#) shows the results obtained for *S. aureus* (G-pos) and *E. coli* (G-neg). Although there was a high envelope-disrupting potential ($81.74\% \pm 8.69\%$) when

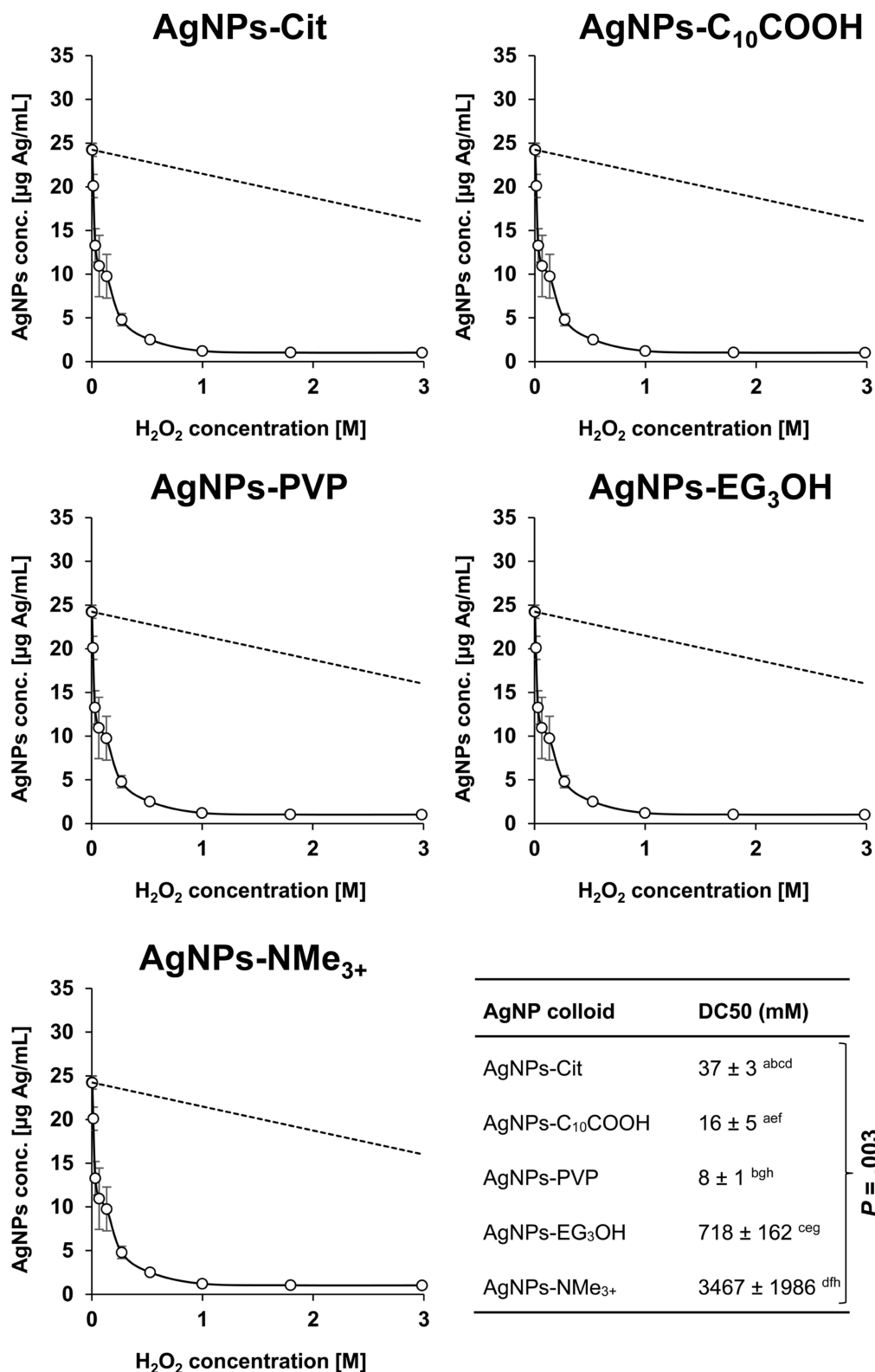


Figure 2 Ligand-dependent dissolution of silver nanoparticles (AgNPs) measured by titration with hydrogen peroxide. DC50, the concentration of hydrogen peroxide dissolving 50% of silver from AgNPs. One-way analysis of variance (ANOVA) followed by the post hoc Tukey’s test was applied to analyze the statistical differences among groups in DC50 value ($P < \alpha$, $\alpha = 0.05$). For further pairwise comparisons, a two-sample t-test was performed. The values with the same letters are significantly different ($P < \alpha$, $\alpha = 0.05$). AgNPs-Cit, AgNPs stabilized with sodium citrate. AgNPs-C₁₀COOH, AgNPs stabilized with mercaptoundecanoic acid. AgNPs-PVP, AgNPs stabilized with polyvinylpyrrolidone. AgNPs-EG₃OH, AgNPs stabilized with triethylene glycol mono-11-mercaptoundecyl ether. AgNPs-NMe₃⁺, AgNPs stabilized with (11-mercaptoundecyl)-N,N,N-trimethylammonium chloride.

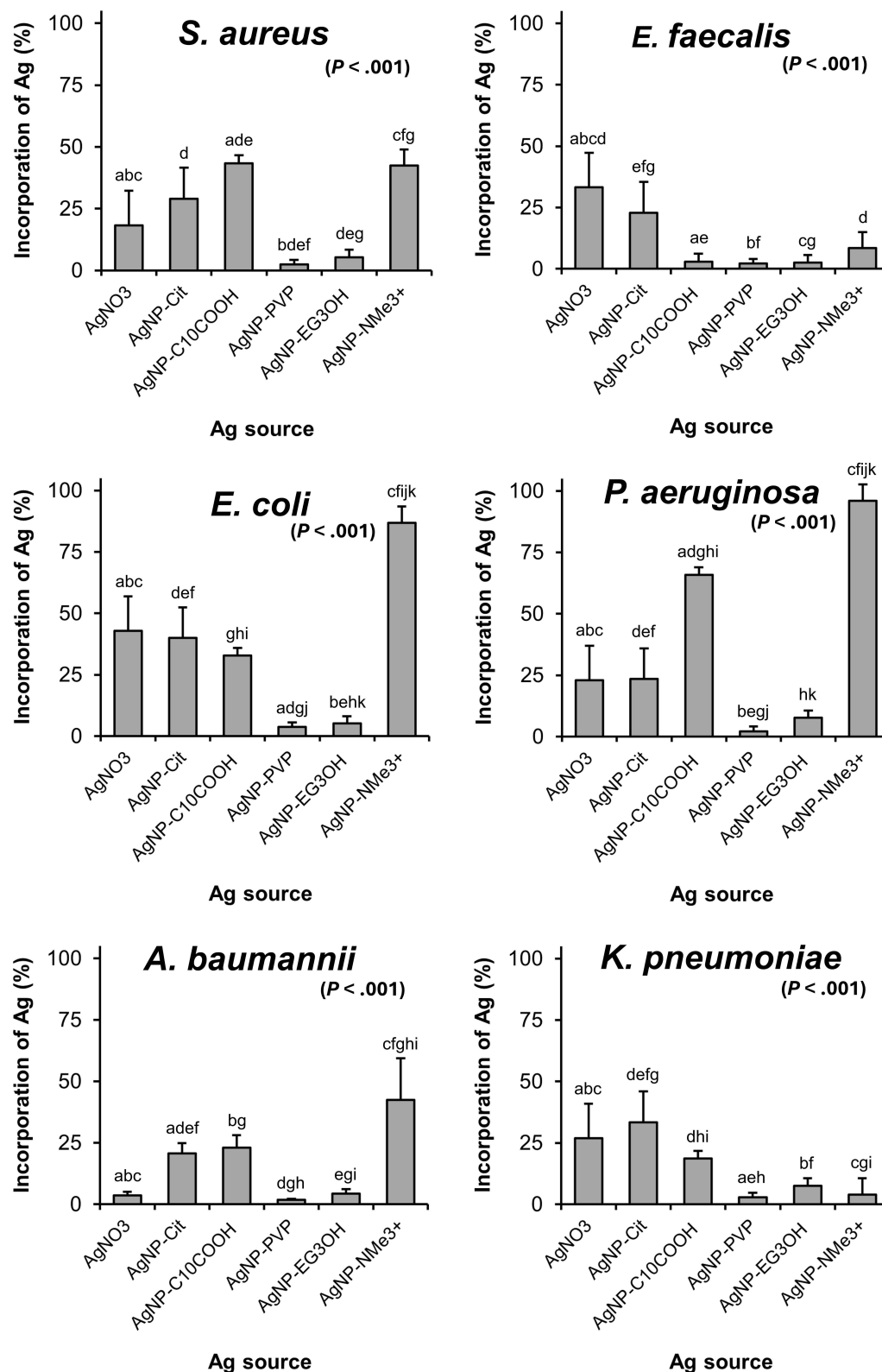


Figure 3 The amount of silver incorporated into bacterial cells from silver nitrate and silver nanoparticles (AgNPs) with distinct surface properties. One-way analysis of variance (ANOVA) followed by the post hoc Tukey's test was applied to analyze differences among silver sources in silver uptake ($P < \alpha$, $\alpha = 0.05$). The values with the same letters are significantly different ($P < \alpha$, $\alpha = 0.05$). AgNPs-Cit, AgNPs stabilized with sodium citrate. AgNPs-C10COOH, AgNPs stabilized with mercaptoundecanoic acid. AgNPs-PVP, AgNPs stabilized with polyvinylpyrrolidone. AgNPs-EG3OH, AgNPs stabilized with triethylene glycol mono-11-mercaptoundecyl ether. AgNPs-NMe₃⁺, AgNPs stabilized with (11-mercaptoundecyl)-N,N,N-trimethylammonium chloride.

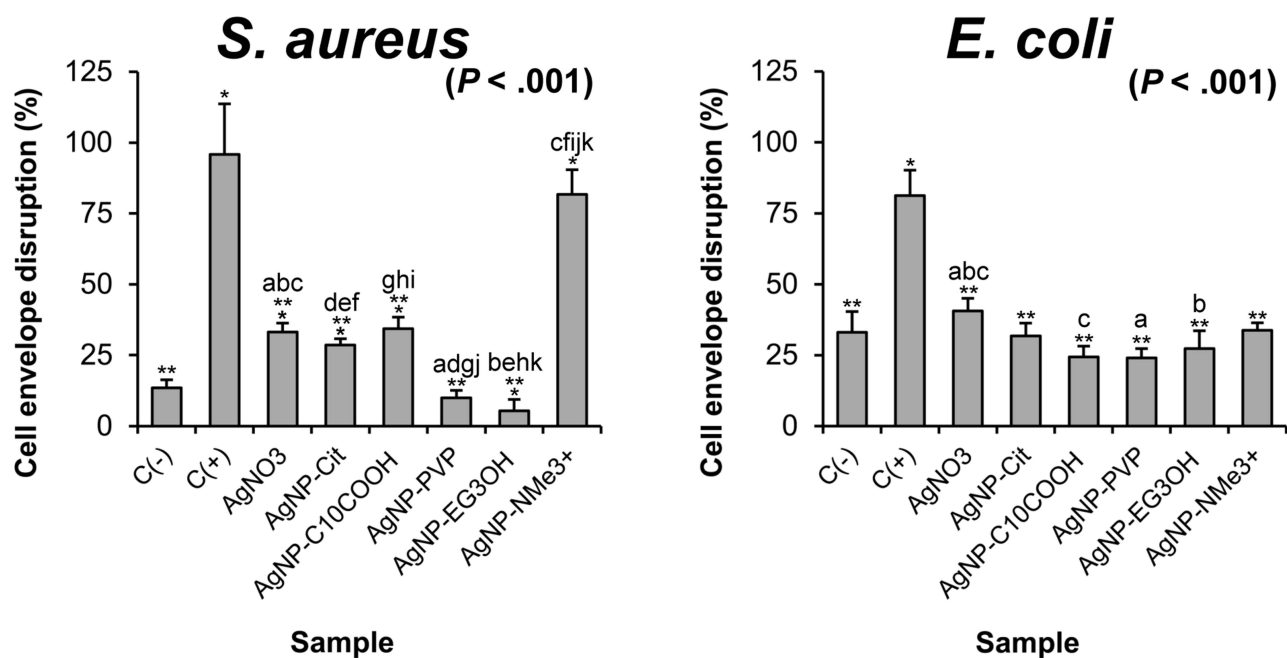


Figure 4 The potential of silver nanoparticles with different surface properties to disrupt the cell envelope of *Staphylococcus aureus* and *Escherichia coli*. C(-), negative control (untreated bacterial cells). C(+), positive control, bacterial cells treated with 0.4 U/mL lysostaphin (*S. aureus*) or 256 µg/mL phenylalanine-arginine β-naphthylamide dihydrochloride (*E. coli*). Statistical significance was analyzed by two-way analysis of variance with post hoc Tukey's test ($P < \alpha$, $\alpha = 0.05$). The means with the same letters are significantly different ($P < \alpha$, $\alpha = 0.05$), whereas values significantly different from negative control and positive control are indicated with the asterisk and double asterisk, respectively. AgNPs-Cit, AgNPs stabilized with sodium citrate. AgNPs-C10COOH, AgNPs stabilized with mercaptoundecanoic acid. AgNPs-PVP, AgNPs stabilized with polyvinylpyrrolidone. AgNPs-EG3OH, AgNPs stabilized with triethylene glycol mono-11-mercaptoundecyl ether. AgNPs-NMe3+, AgNPs stabilized with (11-mercaptoundecyl)-*N,N,N*-trimethylammonium chloride.

we treated *S. aureus* with the positively charged AgNPs-NMe3+, which presented significant antibacterial potential against this pathogen (MIC = 2 µg/mL, MBC = 16 µg/mL), the most active AgNPs-EG3OH (MIC = 1 µg/mL, MBC = 2 µg/mL) caused only 9.98% ± 2.66% cell envelope disruption (Figure 4). Furthermore, moderately active AgNPs-PVP (MIC = 4 µg/mL, MBC = 32 µg/mL) left the bacterial cells nearly intact (Figure 4). Interestingly, the negatively charged AgNPs-Cit and AgNPs-C10COOH, with weak antibacterial potential against *S. aureus* (Figure 1 and Supplementary Table 2), moderately disrupted the cell envelope (Figure 4). When we treated *E. coli* with the tested AgNP colloids, CV uptake did not significantly exceed the level of naturally occurring absorption by untreated bacterial cells (Figure 4). Based on these results, disruption of the bacterial cell envelope is not a determinant of the antibacterial potential of AgNPs.

Structural Changes in Bacterial Cells After Treatment with AgNPs

Next, we visualized changes in bacterial cells after treatment with AgNPs. We selected AgNP-C10COOH as a representative silver source because it led to the most significant differences in antibacterial potential against all of the tested bacterial species (Figure 1). Moreover, the silver absorption from AgNPs-C10COOH was very similar for the species we selected for analysis (G-pos *S. aureus* and G-neg *E. coli*; Figure 3). Representative transmission and scanning electron micrographs are shown in Figures 5 and 6, respectively. *E. coli* treated with nanoparticles showed significant internal changes (Figure 5B), such as cytoplasmic condensation (horizontal arrow) and internal membrane detachment (vertical arrows), which we did not observe in the untreated control (Figure 5A). Although TEM visualization was mostly restricted to intracellular changes, SEM revealed the presence of aggregates covering the bacterial cell surface (Figure 6B, vertical arrows). Moreover, the outer membrane of bacterial cells treated with nanoparticles was not clearly outlined (Figure 6B) compared with that of untreated cells (Figure 6A). In contrast to *E. coli*, *S. aureus* treated with AgNPs-C10COOH did not show pronounced signs of internal disruption (Figure 5D) compared with the untreated control (Figure 5C); we observed only a few intracellular mesosome-like structures²⁶ (Figure 5D, horizontal arrow).

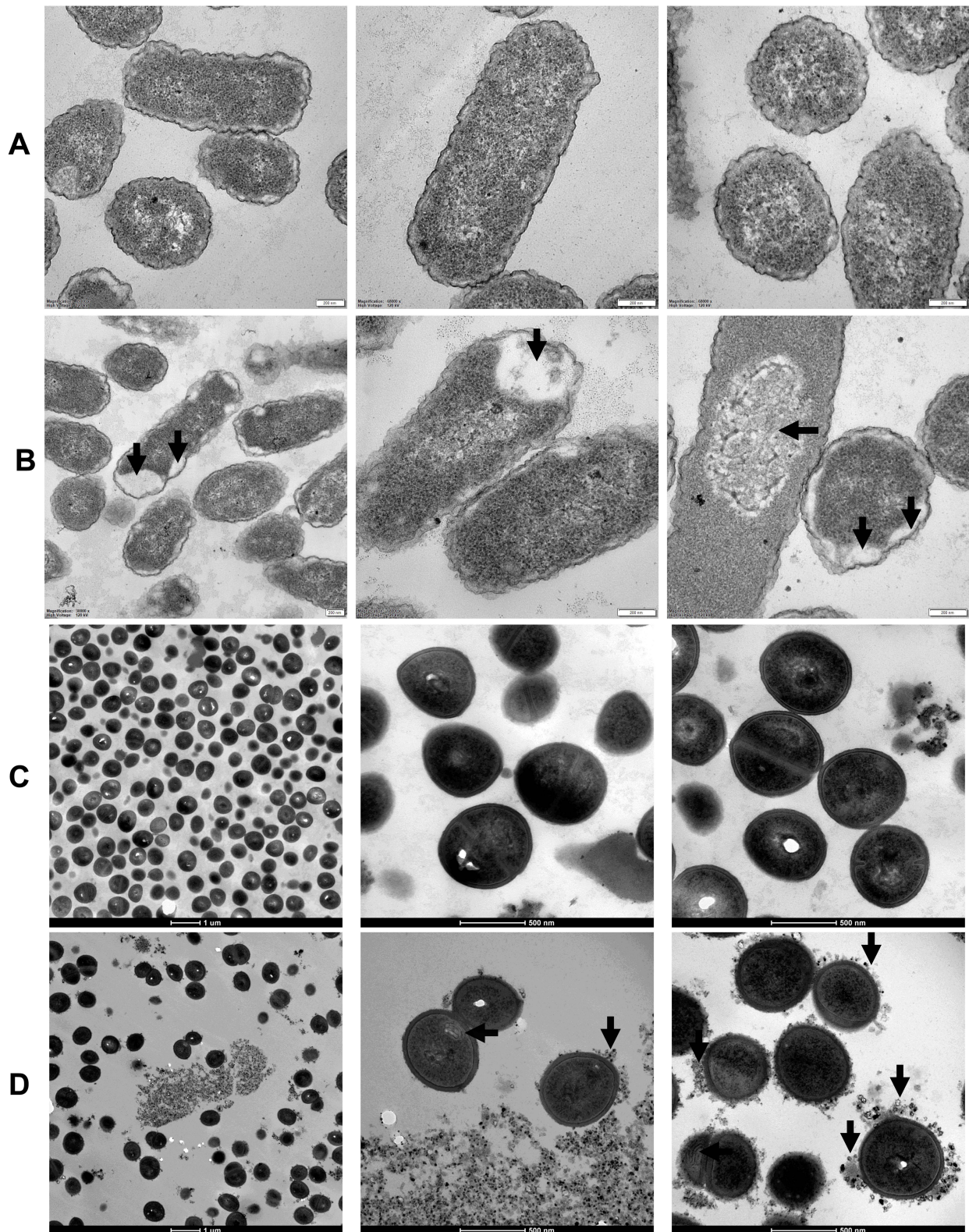


Figure 5 Transmission electron micrographs of model bacterial cells treated with silver nanoparticles. **(A)** Untreated *Escherichia coli*. **(B)** *E. coli* treated with AgNPs-C10COOH (8× the minimal inhibitory concentration [MIC]). **(C)** Untreated *Staphylococcus aureus*. **(D)** *S. aureus* treated with AgNPs-C10COOH (8× MIC). The vertical arrows depict changes observed in the area of the cell envelope, whereas horizontal arrows show intracellular changes. In **(A)** and **(B)**, the white bars represent 200 nm. AgNPs-C10COOH, AgNPs stabilized with mercaptoundecanoic acid.

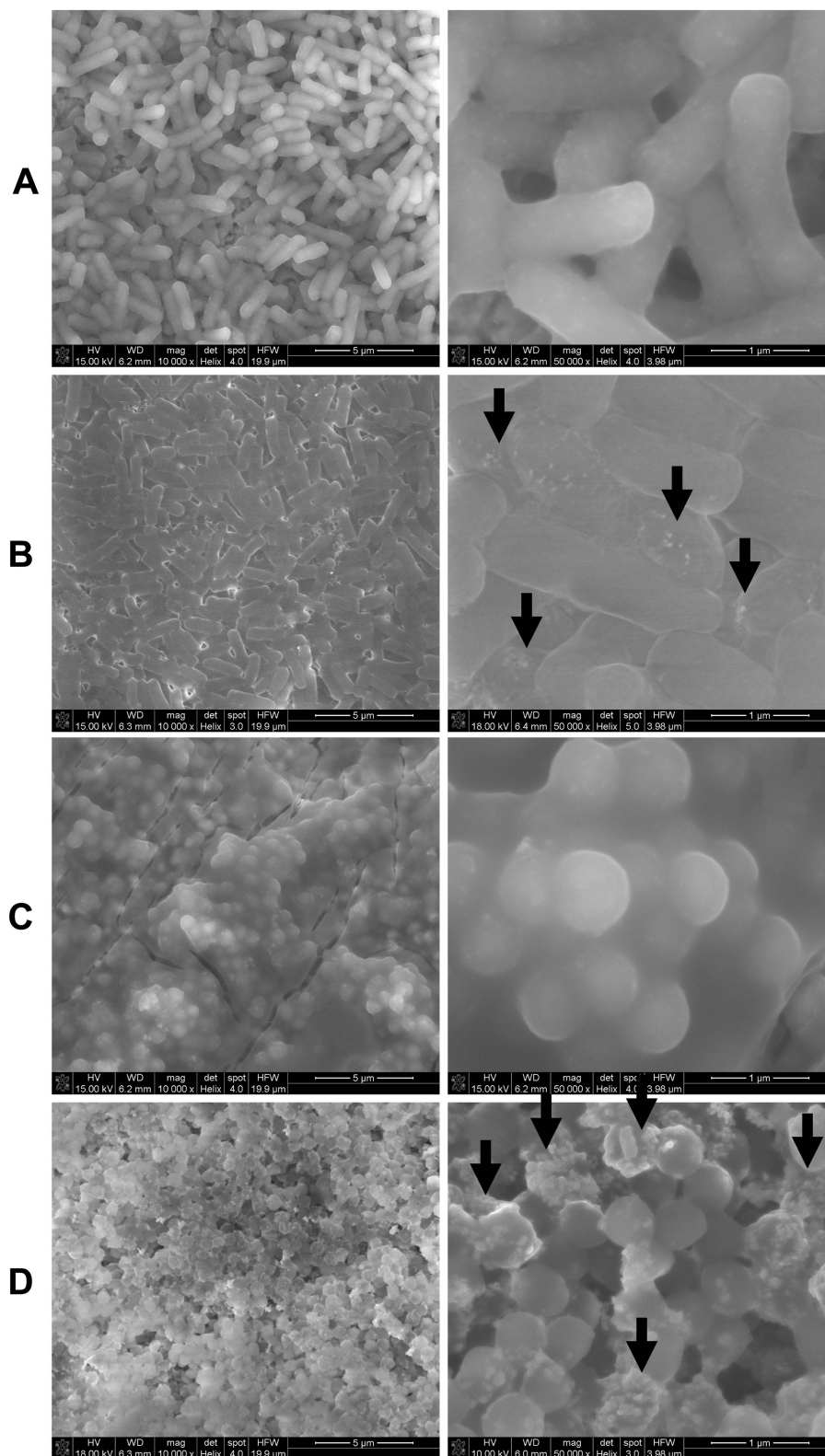


Figure 6 Scanning electron micrographs of model bacterial cells treated with silver nanoparticles. **(A)** Untreated *Escherichia coli*. **(B)** *E. coli* treated with AgNPs-C10COOH (8× the minimal inhibitory concentration [MIC]). **(C)** Untreated *Staphylococcus aureus*. **(D)** *S. aureus* treated with AgNPs-C10COOH (8× MIC). The vertical arrows depict aggregates of AgNPs on the bacterial surface. AgNPs-C10COOH, AgNPs stabilized with mercaptoundecanoic acid.

However, AgNP-C10COOH adhered to the cells and formed a thick layer of aggregates on their surfaces, as visualized by TEM (Figure 5D, vertical arrows) and SEM (Figure 6D, vertical arrows). This clearly demonstrates that the pronounced attachment or aggregation of AgNPs on bacterial cell surfaces is not a determinant of their antibacterial potential.

Hemolytic and Cytotoxic Potential of AgNPs

To examine the interaction between AgNPs and eukaryotic cell membranes, we determined the hemolytic potential of AgNPs in sheep erythrocytes. The nanoparticles with a moderate ζ potential were the most active, leading to cell membrane disruption at significantly lower concentrations than those with highly negative or positive charge (HC50 presented in Supplementary Table 3). Interestingly, the highly cytotoxic silver ions (IC50 = 0.33 ± 0.01 $\mu\text{g Ag/mL}$) were only moderately hemolytic (HC50 = 119 ± 16 $\mu\text{g Ag/mL}$). Next, we performed a preliminary analysis to determine whether selected AgNPs with the opposite surface net charge but corresponding functional groups—that is, positively charged AgNPs-NMe₃⁺ (+68.5 mV) and negatively charged AgNPs-C10COOH (−39.0 mV)—differ in their cytotoxic potential against non-malignant eukaryotic HaCaT cells. These cells remained resistant to AgNPs-C10COOH at a concentration of ≤ 128 $\mu\text{g Ag/mL}$, whereas AgNPs-NMe₃⁺ reduce cell survival by 50% at 59 ± 1 $\mu\text{g Ag/mL}$. Moreover, the analysis confirmed that the nanoparticles are significantly less toxic sources of silver (IC50 in Supplementary Table 3) than the silver salt.

Discussion

In this study, we investigated the antibacterial potential of AgNPs, their attraction to bacterial cells, and their potential to disrupt the cell envelope considering differences in the surface charge of the nanoparticles and bacterial surface properties. Although our findings confirm the unquestionable influence of AgNP surface chemistry on the antibacterial potential, they surprisingly indicate that moderately charged nanoparticles are more active compared with their highly negatively or positively charged counterparts. However, we observed marked variability in the susceptibility to AgNPs among the tested bacterial species and extreme resistance corresponding to the properties of the bacterial cell surface, that is, the presence of an outer cell wall or polysaccharide capsule. Surprisingly, neither enhanced dissolution of nanoparticles nor elevated silver absorption by bacterial cells augmented the antibacterial potential of the tested AgNPs, questioning the crucial role of these two parameters as determinants of the antibacterial potential.

AgNPs are considered to be broad-spectrum antibacterial agents owing to the tremendous number of reports on their activity against bacterial pathogens.^{7,8} However, the results of our study, which we designed to investigate extended ranges of AgNP colloids and bacterial species, challenge this idea. We observed significant differences in susceptibility among the tested bacterial species, as well as examples of significant resistance to AgNPs. Reduced susceptibility of G-pos bacteria to silver has been reported frequently;^{15,27–29} it has been attributed to the presence of a thick cell wall that is hardly permeable to silver ions.⁷ However, we did not expect the reduced sensitivity of *A. baumannii* and significant resistance of *K. pneumoniae*. There have been very few studies on the antibacterial potential of AgNPs against *A. baumannii* and/or *K. pneumoniae* compared with the number of studies involving *E. coli* and *P. aeruginosa*. Although the authors of most of the published reports have concluded that AgNPs have strong antibacterial potential against *A. baumannii* and/or *K. pneumoniae*, the vast majority of studies examined only a single colloid, a very narrow range of AgNP formulations, or a single bacterial strain. However, Porcaro et al¹⁶ clearly observed resistance of both *A. baumannii* and *K. pneumoniae* to negatively charged AgNPs, whereas Wypij et al³⁰ and Mohammed et al³¹ reported reduced susceptibility of *K. pneumoniae* compared with other tested species.

Resistance to silver has been reported mainly for mutants obtained through adaptive laboratory evolution and clinical isolates from environments polluted with silver.^{32,33} Such studies have provided insight into a broad range of adaptive mechanisms, inter alia, silver ion efflux,^{34–36} or an improved response to oxidative stress.³⁷ In our study, all tested bacterial strains were sensitive to ionic silver (MIC ≤ 4 $\mu\text{g/mL}$), and elevated antibacterial doses of selected AgNPs did not correspond with antibacterial doses of silver ions. Hence, the observed bacterial resistance to nanoparticles was not associated with silver ion-dependent mechanisms; rather, it was more likely associated with nanoparticle–cell interactions. The resistance of the G-pos bacteria *S. aureus* and *E. faecalis* indicates the relevance of cell surface properties to

the antibacterial efficacy of AgNPs. The cell envelope of both pathogens consists of a cell membrane enclosed by a thick layer of peptidoglycan with anchored polyanionic teichoic acids and proteins that act as a rigid barrier for molecules and particles.³⁸ The electrostatic attraction between the opposite charges of the cell and nanoparticle can explain the elevated antibacterial potential of highly positively charged AgNPs (+68.5 mV) against *S. aureus* and *E. faecalis*. However, the properties of moderately charged AgNPs (−21.5 mV and +14.9 mV)—that is, the highest antibacterial potential and the lowest absorption into bacterial cells—suggest a more sophisticated mechanism of the interaction with the cell. Such a conclusion is also supported by the results for the G-neg *K. pneumoniae*, which is covered by a thick polysaccharide capsule (Supplementary Figure 3) with a strong anionic charge and is more susceptible to moderately and highly positively charged AgNPs compared with their negatively charged counterparts. Recently, Panáček et al³⁹ and Yang et al⁴⁰ reported that microbial exopolysaccharides, which bind and inactivate AgNPs or silver ions, are responsible for bacterial resistance to AgNPs.

The shape, size, and surface properties of AgNPs are extremely relevant for their biological potential.^{2,3,8,13} Frequently applied and easily available spherical nanoparticles are considered to be the most potent nanoparticles after triangles, platelets, and nanorods, all of which have a very large contact surface.^{41–44} The significance of size for antibacterial activity has been reiterated in many reports, but a systematic study on uniform, 5–100 nm nanoparticles synthesized with the same method and capped with the same ligand provided substantial insight into this matter.⁴⁵ Although the results confirmed that the inhibitory and bactericidal potential of AgNPs decreased as the nanoparticle size increased, a 2-fold difference in the MIC or MBC required a 4–10-fold difference in the diameter.⁴⁵ In another study, there was a correlation between increasing size and reduced antibacterial potential, a phenomenon that can be explained by the slower dissolution of silver ions from larger AgNPs.⁴⁶ Although we used uniform AgNPs in our study, thorough analyses revealed that the size of one of tested colloids was < 5 nm. Nevertheless, the reduced size did not contribute to an overall higher antibacterial potential compared with other studied colloids with a diameter around 5 nm. These findings confirm the relevance of the nanoparticle surface properties for the antibacterial activity of AgNPs.

It is largely accepted that the surface charge of nanoparticles, described by the ζ potential, defines the stability of colloids and their interaction with cells and the surrounding environment.¹³ According to the literature, the high absolute ζ potential of AgNPs (below −30 mV and above +30 mV) indicates excellent stability of the colloid.⁴⁷ In contrast to previous reports, we did not observe significant aggregation of the tested colloids in water or when applying an elevated temperature, despite studying AgNPs with a broad ζ potential range (from −47.6 mV to +68.5 mV). In fact, we only noted a correlation between the ζ potential and another aspect of colloidal stability, that is, positively charged AgNPs were resistant to the dissolution of silver ions.

We introduced bacterial cells into the medium immediately after the AgNP colloids, thus minimizing the interaction between AgNPs and medium components. It is worth noting that the pH of the medium was slightly basic pH (7.3) and close to the pH of ultrapure water used to determine colloidal stability and the ζ potential. Moreover, we assumed that the applied medium reflects wound conditions, that is, the target of antibacterial AgNPs, where protein and peptides potentially altering the properties of AgNPs and influencing their biological activity are present. Hence, we did not measure the ζ potential and colloidal stability in culture medium. However, we must emphasize that the parameters of the medium, including the pH and ionic strength, as well as the biomolecules present in the environment can alter the stability and biological potential of AgNPs. In previous studies, the ζ potential of nanoparticles coated with citrate changed in biological media but remained negative.^{48,49} Although citrate stabilized AgNPs incubated in biological media aggregate significantly,^{49,50} according to Bélteky et al,⁴⁹ their aggregation accelerated after incubation for 1.5 h. The surface net charge of AgNPs capped with mercaptoundecanoic acid increased at basic pH or decreased at acidic pH (remaining negative), but was not significantly impacted by ionic strength of medium.⁵¹ On the other hand, when Long et al⁵² incubated mercaptoundecanoic acid-AgNPs in mouse plasma, they presented a stable ζ potential and no significant changes in their size distribution. Among others, Tejamaya et al⁵⁰ showed that AgNPs stabilized with PVP or polyethylene glycol (PEG) are less affected by medium and aggregate only slightly compared to citrate-stabilized AgNP. Moreover, PVP and PEG are polymers that resist protein absorption when covering the surface of nanoparticle.⁵³ Pucelik et al⁵⁴ reported that AgNPs stabilized with (11-mercaptoundecyl)-*N,N,N*-trimethylammonium chloride remain stable in Dulbecco's Modified Eagle Medium for up to 5 days.

The authors of many previous reports have attributed the high antibacterial activity of AgNPs to their high ζ potential—that is, a highly positive net charge—which the authors claimed were responsible for the electrostatic attraction between nanoparticles and bacterial cell envelope.^{51–54} By contrast, Lin et al¹⁴ found superior antibacterial activity of highly negatively charged AgNPs against *E. coli*, Bondarenko et al¹⁵ reported that AgNPs with moderate negative charge were the most active against multiple bacterial strains, and Porcaro et al¹⁶ noted highly negatively charged AgNPs were the most potent against selected ESKAPE pathogens. In contrast to the previous reports, we used nanoparticles characterized by a broad ζ potential and demonstrated that moderately charged AgNPs ($\zeta = -21.5$ mV or $+14.9$ mV) possessed significantly higher antibacterial activity toward most of the tested pathogens compared with highly negatively charged AgNPs ($\zeta = -47.6$ mV and -39 mV) or highly positively charged AgNPs ($\zeta = +68.5$ mV).

The bimodal antibacterial mechanism of AgNPs, which is based on high reactivity of silver ions and nanoparticle–cell interactions, is widely accepted.⁷ Silver ions lead to bacterial cell death through the interaction with multiple proteins and the interference with many housekeeping cellular processes leading to multi-layer changes.⁵⁵ In contrast to previous studies,^{41,56–58} we did not observe a correlation between susceptibility to the dissolution of silver ions and antibacterial potential of AgNPs. Hence, the role of silver ions released from nanoparticles in the medium is not substantial for the antibacterial activity of the tested AgNP colloids. Antibacterial activity that depends on nanoparticle–cell interactions involves the following events: (i) AgNP attachment to the bacterial cell envelope, (ii) cell membrane damage, and (iii) cell entrance and interaction with biomolecules.^{7,8,18,57,59} Our study indicates that while AgNPs attach to bacterial cells and destabilize the cell envelope, these events do not contribute to their antibacterial potential. Moreover, the most active AgNPs were two poorly absorbed colloids with a moderate surface charge, so our results highlight that AgNPs need to be internalized and interact with intracellular biomolecules to exert their antibacterial effect.

Interestingly, analyses performed on model membranes of eukaryotic cells (ie, sheep erythrocytes) suggested a strong interaction between the cells and highly negatively or moderately charged nanoparticles, leading to membrane disruption. Surprisingly, positively charged AgNPs with a slight hemolytic potential were more cytotoxic compared than their non-hemolytic, negatively charged counterparts. The relationship between the interaction with eukaryotic cell membranes and cytotoxicity has been reported in many previous studies.⁶⁰ However, our results also indicate that the cytotoxicity does not result simply from the interaction with cell membranes.

Although this study is the first to describe the complexity of the interaction between biological and nanoparticle surfaces and its impact on biological activity, it had a few limitations. First, the study design and applied methods did not allow us to distinguish between AgNPs incorporated into the cells and those that adhered to the bacterial surface. The relationship between the antibacterial potential of nanoparticles and the amount of bioavailable silver interacting with cellular components should be addressed in future research. Second, we did not characterize the chemistry and properties of the bacterial cell surfaces, which, according to our results, allows nanoparticle sequestration on bacterial surfaces and inhibits their potential. Because the surface properties can differ among bacterial species and strains, it is pivotal to determine the chemical markers that influence the antibacterial potential of AgNP colloids. Third, based on our justified assumptions, we simplified the model and analyzed nanoparticle surface properties and size distribution in water. However, the interaction of nanoparticles of varying surface properties with the medium or surrounding environment is a starting point for further investigation. Finally, to investigate the possible mechanism underlying the antibacterial activity of AgNPs, we applied methods based on spectrometry, which questioned the relevance of the effects that have been described in the literature. In the future, it is essential to apply molecular methods and omics technologies to understand the events that lead to bacterial growth inhibition and cell death.

Conclusion

In summary, the results of this study indicate that the antibacterial potential of AgNPs is the result of the interplay between nanoparticles and the cell surface. A moderate surface net charge is crucial to reduce excess attachment of nanoparticles to the bacterial cell surface and to allow cell infiltration by silver nanoparticles. Intrinsic cellular barriers, that is, the cell wall and surface polysaccharides, significantly reduce the potential of nanoparticles. According to our results, neither dissolution of silver ions nor absorption on the cell surface and disruption of the cell envelope determine the antibacterial potential of AgNPs. Rather, their efficacy rely on entry into bacterial cells.

Data Sharing Statement

The data for this study are available at the BRIDGE of Knowledge repository (Gdansk University of Technology) at <https://doi.org/10.34808/97fn-xr10>.

Acknowledgments

The authors are very grateful to Malwina Richert, a former technician at the Laboratory of Electron Microscopy, Faculty of Biology, University of Gdansk, for performing the TEM analyses.

Author Contributions

All authors made a significant contribution to the work reported, whether that is in the conception, study design, execution, acquisition of data, analysis and interpretation, or in all these areas; took part in drafting, revising or critically reviewing the article; gave final approval of the version to be published; have agreed on the journal to which the article has been submitted; and agree to be accountable for all aspects of the work.

Current Affiliation

Karolina Bogaj: Laboratory of Electrophysiology, Nencki Institute of Experimental Biology, Polish Academy of Sciences, Warsaw, Poland.

Ewa Czechowska: Faculty of Chemistry, University of Wrocław, Warsaw, Poland.

Funding

This work was financially supported by the Program of Small Grants Ugrants-start (project no. 533-N000-GS12-22 granted to MKM) at the University of Gdansk (Initiative for Research University Excellence, IDUB), and by the Ministry of Education and Science of Poland as part of a research subsidy to the University of Gdansk (no. 531-N104-D800-23).

Disclosure

The authors report no conflicts of interest in this work.

References

1. Al-Radadi NS, Abu-Dief AM. Silver nanoparticles (AgNPs) as a metal nano-therapy: possible mechanisms of antiviral action against COVID-19. *Inorg Nanomet Chem.* 2022;1–19. doi:10.1080/24701556.2022.2068585
2. Tang S, Zheng J. Antibacterial activity of silver nanoparticles: structural effects. *Adv Healthc Mater.* 2018;7(13). doi:10.1002/adhm.201701503
3. Zhang J, Wang F, Yalamarty SSK, Filipczak N, Jin Y, Li X. Nano silver-induced toxicity and associated mechanisms. *Int J Nanomed.* 2022;26(17):1851–1864. doi:10.2147/IJN.S355131
4. Qamer S, Romli MH, Che-Hamzah F, et al. Systematic review on biosynthesis of silver nanoparticles and antibacterial activities: application and theoretical perspectives. *Molecules.* 2021;26(16):5057. doi:10.3390/molecules26165057
5. Gurnathan S, Choi YJ, Kim JH. Antibacterial efficacy of silver nanoparticles on endometritis caused by *Prevotella melaninogenica* and *Arcanobacterium pyogenes* in dairy cattle. *Int J Mol Sci.* 2018;19(4):1210. doi:10.3390/ijms19041210
6. Mishra S, Singh HB. Biosynthesized silver nanoparticles as a nanoweapon against phytopathogens: exploring their scope and potential in agriculture. *Appl Microbiol Biotechnol.* 2015;99(3):1097–1107. doi:10.1007/s00253-014-6296-0
7. Qing Y, Cheng L, Li R, et al. Potential antibacterial mechanism of silver nanoparticles and the optimization of orthopedic implants by advanced modification technologies. *Int J Nanomed.* 2018;13:3311–3327. doi:10.2147/IJN.S165125
8. Tripathi N, Goshisht MK. Recent advances and mechanistic insights into antibacterial activity, antibiofilm activity, and cytotoxicity of silver nanoparticles. *ACS Appl Bio Mater.* 2022;5(4):1391–1463. doi:10.1021/acsabm.2c00014
9. Liu B, Liu D, Chen T, et al. iTRAQ-based quantitative proteomic analysis of the antibacterial mechanism of silver nanoparticles against multidrug-resistant *Streptococcus suis*. *Front Microbiol.* 2023;14:1293363. doi:10.3389/fmicb.2023.1293363
10. Hurd T, Woodmansey EJ, Watkins HMA. A retrospective review of the use of a nanocrystalline silver dressing in the management of open chronic wounds in the community. *Int Wound J.* 2021;18(6):753–762. doi:10.1111/iwj.13576
11. Dissemmond J, Bottrich JG, Braunwarth H, Hilt J, Wilken P, Munter KC. Evidence for silver in wound care - meta-analysis of clinical studies from 2000–2015. *J Dtsch Dermatol Ges.* 2017;15(5):524–535. doi:10.1111/ddg.13233
12. Las Heras K, Igartua M, Santos-Vizcaino E, Hernandez RM. Chronic wounds: current status, available strategies and emerging therapeutic solutions. *J Control Release.* 2020;328:532–550. doi:10.1016/j.jconrel.2020.09.039
13. Restrepo CV, Villa CC. Synthesis of silver nanoparticles, influence of capping agents, and dependence on size and shape: a review. *Environ Nanotechnol Monit Manag.* 2021;15:100428. doi:10.1016/j.enmm.2021.100428
14. Lin JJ, Lin WC, Dong RX, Hsu S. The cellular responses and antibacterial activities of silver nanoparticles stabilized by different polymers. *Nanotechnology.* 2012;23(6):065102. doi:10.1088/0957-4484/23/6/065102

15. Bondarenko O, Ivask A, Käkinen A, Kurvet I, Kahru A. Particle-cell contact enhances antibacterial activity of silver nanoparticles. *PLoS One*. 2013;8(5):e64060. doi:10.1371/journal.pone.0064060
16. Porcaro F, Carlini L, Ugolini A, et al. Synthesis and structural characterization of silver nanoparticles stabilized with 3-mercaptopropylsulfonate and 1-thiogluconate mixed thiols for antibacterial applications. *Materials*. 2016;9(12):1028. doi:10.3390/ma9121028
17. Ivask A, ElBadawy A, Kaweeteerawut C, et al. Toxicity mechanisms in *Escherichia coli* vary for silver nanoparticles and differ from ionic silver. *ACS Nano*. 2014;8(1):374–386. doi:10.1021/nn4044047
18. El Badawy AM, Silva RG, Morris B, Scheckel KG, Suidan MT, Tolaymat TM. Surface charge-dependent toxicity of silver nanoparticles. *Environ Sci Technol*. 2011;45(1):283–287. doi:10.1021/es1034188
19. Dai X, Chen X, Zhao J, et al. Structure–activity relationship of membrane-targeting cationic ligands on a silver nanoparticle surface in an antibiotic-resistant antibacterial and antibiofilm activity assay. *ACS Appl Mater Interfaces*. 2017;9(16):13837–13848. doi:10.1021/acsami.6b15821
20. Abbaszadegan A, Ghahramani Y, Gholami A, et al. The effect of charge at the surface of silver nanoparticles on antimicrobial activity against gram-positive and gram-negative bacteria: a preliminary study. *J Nanomater*. 2015;2015:1–8. doi:10.1155/2015/720654
21. Bengoechea JA, Sa Pessoa J. *Klebsiella pneumoniae* infection biology: living to counteract host defences. *FEMS Microbiol Rev*. 2019;43(2):123–144. doi:10.1093/femsre/fuy043
22. Krychowiak-Maśnicka M, Krauze-Baranowska M, Godlewska S, et al. Potential of silver nanoparticles in overcoming the intrinsic resistance of *Pseudomonas aeruginosa* to secondary metabolites from carnivorous plants. *Int J Mol Sci*. 2021;22(9):4849. doi:10.3390/ijms22094849
23. Ho CM, Yau SKW, Lok CN, So MH, Che CM. Oxidative dissolution of silver nanoparticles by biologically relevant oxidants: a kinetic and mechanistic study. *Chem Asian J*. 2010;5(2):285–293. doi:10.1002/asia.200900387
24. Halder S, Yadav KK, Sarkar R, et al. Alteration of zeta potential and membrane permeability in bacteria: a study with cationic agents. *Springerplus*. 2015;4:672. doi:10.1186/s40064-015-1476-7
25. Zhao Y, Sun X, Zhang G, Trewyn BG, Slowing II, Lin VSY. Interaction of mesoporous silica nanoparticles with human red blood cell membranes: size and surface effects. *ACS Nano*. 2011;5(2):1366–1375. doi:10.1021/nn103077k
26. Krychowiak M, Kawiak A, Narajczyk M, Borowik A, Krolicka A. Silver nanoparticles combined with naphthoquinones as an effective synergistic strategy against *Staphylococcus aureus*. *Front Pharmacol*. 2018;9:9. doi:10.3389/fphar.2018.00816
27. Feng QL, Wu J, Chen GQ, Cui FZ, Kim TN, Kim JO. A mechanistic study of the antibacterial effect of silver ions on *Escherichia coli* and *Staphylococcus aureus*. *J Biomed Mater Res*. 2000;52(4):662–668. doi:10.1002/1097-4636(20001215)52:4<662::Aid-Jbm10>3.0.Co;2-3
28. Chen Y, Sun W, Qu D, Ma Y, Liu C, Zhou J. Enhanced stability and antibacterial efficacy of a traditional Chinese medicine-mediated silver nanoparticle delivery system. *Int J Nanomed*. 2014;9:5491–5502. doi:10.2147/IJN.S71670
29. Siddiq AM, Parandhman T, Begam AF, Das SK, Alam MS. Effect of Gemini surfactant (16-6-16) on the synthesis of silver nanoparticles: a facile approach for antibacterial application. *Enzyme Microb Technol*. 2016;95:118–127. doi:10.1016/j.enzmictec.2016.08.009
30. Wypij M, Czarnecka J, Świecimska M, Dahm H, Rai M, Golinska P. Synthesis, characterization and evaluation of antimicrobial and cytotoxic activities of biogenic silver nanoparticles synthesized from *Streptomyces xinghaiensis* OF1 strain. *World J Microbiol Biotechnol*. 2018;34(2):23. doi:10.1007/s11274-017-2406-3
31. Mohammed AE, Alghamdi SS, Shami A, et al. In silico prediction of *Malvaviscus arboreus* metabolites and green synthesis of silver nanoparticles – opportunities for safer anti-bacterial and anti-cancer precision medicine. *Int J Nanomed*. 2023;18:2141–2162. doi:10.2147/IJN.S400195
32. Salas-Orozco MF, Lorenzo-Leal AC, de Alba Montero I, Marín NP, Santana MAC, Bach H. Mechanism of escape from the antibacterial activity of metal-based nanoparticles in clinically relevant bacteria: a systematic review. *Nanomedicine*. 2024;55:102715. doi:10.1016/j.nano.2023.102715
33. Mijndonckx K, Leys N, Mahillon J, Silver S, Van Houdt R. Antimicrobial silver: uses, toxicity and potential for resistance. *Biometals*. 2013;26(4):609–621. doi:10.1007/s10534-013-9645-z
34. Stabryla LM, Johnston KA, Diemler NA, et al. Role of bacterial motility in differential resistance mechanisms of silver nanoparticles and silver ions. *Nat Nanotechnol*. 2021;16(9):996–1003. doi:10.1038/s41565-021-00929-w
35. Franke S, Grass G, Nies DH. The product of the ybdE gene of the *Escherichia coli* chromosome is involved in detoxification of silver ions. *Microbiology*. 2001;147(4):965–972. doi:10.1099/00221287-147-4-965
36. Gupta A, Matsui K, Lo JF, Silver S. Molecular basis for resistance to silver cations in *Salmonella*. *Nat Med*. 1999;5(2):183–188. doi:10.1038/5545
37. Valentin E, Bottomley AL, Chilambi GS, et al. Heritable nanosilver resistance in priority pathogen: a unique genetic adaptation and comparison with ionic silver and antibiotics. *Nanoscale*. 2020;12(4):2384–2392. doi:10.1039/C9NR08424J
38. Neuhaus FC, Baddiley J. A Continuum of anionic charge: structures and functions of D-alanyl-teichoic acids in gram-positive bacteria. *Microbiol Mol Biol Rev*. 2003;67(4):686–723. doi:10.1128/MMBR.67.4.686-723.2003
39. Panáček A, Kvítel L, Šmákalová M, et al. Bacterial resistance to silver nanoparticles and how to overcome it. *Nat Nanotechnol*. 2018;13(1):65–71. doi:10.1038/s41565-017-0013-y
40. Yang Y, Chen X, Zhang N, et al. Self-defense mechanisms of microorganisms from the antimicrobial effect of silver nanoparticles: highlight the role of extracellular polymeric substances. *Water Res*. 2022;218:118452. doi:10.1016/j.watres.2022.118452
41. Helmlinger J, Sengstock C, Groß-Heitfeld C, et al. Silver nanoparticles with different size and shape: equal cytotoxicity, but different antibacterial effects. *RSC Adv*. 2016;6(22):18490–18501. doi:10.1039/C5RA27836H
42. Pal S, Tak YK, Song JM. Does the antibacterial activity of silver nanoparticles depend on the shape of the nanoparticle? A study of the gram-negative bacterium *Escherichia coli*. *Appl Environ Microbiol*. 2007;73(6):1712–1720. doi:10.1128/AEM.02218-06
43. Stabryla LM, Moncure PJ, Millstone JE, Gilbertson LM. Particle-driven effects at the bacteria interface: a nanosilver investigation of particle shape and dose metric. *ACS Appl Mater Interfaces*. 2023;15(33):39027–39038. doi:10.1021/acsami.3c00144
44. Omar R, Ibraheem IBM, Hassan S, Elsayed KNM. Biogenic synthesis of different forms of bio-capped silver nanoparticles using *Microcystis* sp. and its antimicrobial activity. *Curr Nanosci*. 2023;19(6):850–862. doi:10.2174/1573413719666230202122334
45. Agnihotri S, Mukherji S, Mukherji S. Size-controlled silver nanoparticles synthesized over the range 5–100 nm using the same protocol and their antibacterial efficacy. *RSC Adv*. 2014;4(8):3974–3983. doi:10.1039/C3RA44507K
46. Zhang W, Yao Y, Sullivan N, Chen Y. Modeling the primary size effects of citrate-coated silver nanoparticles on their ion release kinetics. *Environ Sci Technol*. 2011;45(10):4422–4428. doi:10.1021/es104205a

47. Badawy A, Luxton TP, Silva RG, Scheckel KG, Suidan MT, Tolaymat TM. Impact of environmental conditions (pH, ionic strength, and electrolyte type) on the surface charge and aggregation of silver nanoparticles suspensions. *Environ Sci Technol*. 2010;44(4):1260–1266. doi:10.1021/es902240k
48. Srivastava P, Gunawan C, Soeriyadi A, Amal R, Hoehn K, Marquis C. In vitro coronal protein signatures and biological impact of silver nanoparticles synthesized with different natural polymers as capping agents. *Nanoscale Adv*. 2021;3(15):4424–4439. doi:10.1039/D0NA01013H
49. Béteky P, Rónavári A, Zakupszky D, et al. Are smaller nanoparticles always better? Understanding the biological effect of size-dependent silver nanoparticle aggregation under biorelevant conditions. *Int J Nanomed*. 2021;16:3021–3040. doi:10.2147/IJN.S304138
50. Tejamaya M, Römer I, Merrifield RC, Lead JR. Stability of citrate, PVP, and PEG coated silver nanoparticles in ecotoxicology media. *Environ Sci Technol*. 2012;46(13):7011–7017. doi:10.1021/es2038596
51. Dougherty GM, Rose KA, Tok JB–H, et al. The zeta potential of surface-functionalized metallic nanorod particles in aqueous solution. *Electrophoresis*. 2008;29(5):1131–1139. doi:10.1002/elps.200700448
52. Long YM, Zhao XC, Clermont AC, et al. Negatively charged silver nanoparticles cause retinal vascular permeability by activating plasma contact system and disrupting adherens junction. *Nanotoxicology*. 2016;10(4):501–511. doi:10.3109/17435390.2015.1088589
53. Holmlin RE, Chen X, Chapman RG, Takayama S, Whitesides GM. Zwitterionic SAMs that resist nonspecific adsorption of protein from aqueous buffer. *Langmuir*. 2001;17(9):2841–2850. doi:10.1021/la0015258
54. Pucelik B, Sulek A, Borkowski M, Barzowska A, Kobielski M, Dąbrowski JM. Synthesis and characterization of size- and charge-tunable silver nanoparticles for selective anticancer and antibacterial treatment. *ACS Appl Mater Interfaces*. 2022;14(13):14981–14996. doi:10.1021/acsami.2c01100
55. Wang H, Yan A, Liu Z, et al. Deciphering molecular mechanism of silver by integrated omic approaches enables enhancing its antimicrobial efficacy in *E. coli*. *PLoS Biol*. 2019;17(6):e3000292. doi:10.1371/journal.pbio.3000292
56. Liu J, Sonshine DA, Shervani S, Hurt RH. Controlled release of biologically active silver from nanosilver surfaces. *ACS Nano*. 2010;4(11):6903–6913. doi:10.1021/nn102272n
57. Dai X, Guo Q, Zhao Y, et al. Functional silver nanoparticle as a benign antimicrobial agent that eradicates antibiotic-resistant bacteria and promotes wound healing. *ACS Appl Mater Interfaces*. 2016;8(39):25798–25807. doi:10.1021/acsami.6b09267
58. Sorinolu AJ, Godakhindi V, Siano P, Vivero-Escoto JL, Munir M. Influence of silver ion release on the inactivation of antibiotic resistant bacteria using light-activated silver nanoparticles. *Mater Adv*. 2022;3(24):9090–9102. doi:10.1039/D2MA00711H
59. Ferreyra Maillard APV, Dalmaso PR, López de Mishima BA, Hollmann A. Interaction of green silver nanoparticles with model membranes: possible role in the antibacterial activity. *Colloids Surf B Biointerfaces*. 2018;171:320–326. doi:10.1016/j.colsurfb.2018.07.044
60. Leroueil PR, Hong S, Mecke A, Baker JR, Orr BG, Banaszak Holl MM. Nanoparticle interaction with biological membranes: does nanotechnology present a Janus face? *Acc Chem Res*. 2007;40(5):335–342. doi:10.1021/ar600012y

Nanotechnology, Science and Applications

Dovepress

Publish your work in this journal

Nanotechnology, Science and Applications is an international, peer-reviewed, open access journal that focuses on the science of nanotechnology in a wide range of industrial and academic applications. It is characterized by the rapid reporting across all sectors, including engineering, optics, bio-medicine, cosmetics, textiles, resource sustainability and science. Applied research into nano-materials, particles, nano-structures and fabrication, diagnostics and analytics, drug delivery and toxicology constitute the primary direction of the journal. The manuscript management system is completely online and includes a very quick and fair peer-review system, which is all easy to use. Visit <http://www.dovepress.com/testimonials.php> to read real quotes from published authors.

Submit your manuscript here: <https://www.dovepress.com/nanotechnology-science-and-applications-journal>